



## The $\beta$ -decay of $^{70}\text{Kr}$ into $^{70}\text{Br}$ : Restoration of the pseudo-SU(4) symmetry



A. Vitéz-Sveicz <sup>a,b,c</sup>, A. Algóra <sup>a,b</sup>, A.I. Morales <sup>a</sup>, B. Rubio <sup>a</sup>, G.G. Kiss <sup>b,d,\*</sup>, P. Sarriguren <sup>e</sup>, P. Van Isacker <sup>f</sup>, G. de Angelis <sup>g</sup>, F. Recchia <sup>h,i</sup>, S. Nishimura <sup>d</sup>, J. Agramunt <sup>a</sup>, V. Guadilla <sup>a</sup>, A. Montaner-Pizá <sup>a</sup>, S.E.A. Orrigo <sup>a</sup>, A. Horváth <sup>j</sup>, D. Napoli <sup>g</sup>, S. Lenzi <sup>h,i</sup>, A. Boso <sup>h,i</sup>, V.H. Phong <sup>d,k</sup>, J. Wu <sup>d</sup>, P.-A. Söderström <sup>l</sup>, T. Sumikama <sup>d</sup>, H. Suzuki <sup>d</sup>, H. Takeda <sup>d</sup>, D.S. Ahn <sup>d</sup>, H. Baba <sup>d</sup>, P. Doornebal <sup>d</sup>, N. Fukuda <sup>d</sup>, N. Inabe <sup>d</sup>, T. Isobe <sup>d</sup>, T. Kubo <sup>d</sup>, S. Kubono <sup>d</sup>, H. Sakurai <sup>d</sup>, Y. Shimizu <sup>d</sup>, C. Sidong <sup>d</sup>, B. Blank <sup>m</sup>, P. Ascher <sup>m</sup>, M. Gerbaux <sup>m</sup>, T. Goigoux <sup>m</sup>, J. Giovinazzo <sup>m</sup>, S. Grévy <sup>m</sup>, T. Kurtukián Nieto <sup>m</sup>, C. Magron <sup>m</sup>, W. Gelletly <sup>a,n</sup>, Zs. Dombrádi <sup>b</sup>, Y. Fujita <sup>o,p</sup>, M. Tanaka <sup>p</sup>, P. Aguilera <sup>q</sup>, F. Molina <sup>q</sup>, J. Eberth <sup>r</sup>, F. Diel <sup>r</sup>, D. Lubos <sup>s</sup>, C. Borcea <sup>t</sup>, E. Ganioglu <sup>u</sup>, D. Nishimura <sup>v</sup>, H. Oikawa <sup>w</sup>, Y. Takei <sup>w</sup>, S. Yagi <sup>w</sup>, W. Korten <sup>x</sup>, G. de France <sup>y</sup>, P. Davies <sup>z</sup>, J. Liu <sup>aa</sup>, J. Lee <sup>aa</sup>, T. Lokotko <sup>aa</sup>, I. Kojouharov <sup>ab</sup>, N. Kurz <sup>ab</sup>, H. Shaffner <sup>ab</sup>, A. Petrovici <sup>t</sup>

<sup>a</sup> Instituto de Física Corpuscular, CSIC-Universitat de València, E-46071 València, Spain

<sup>b</sup> Institute for Nuclear Research (Atomki), H-4001 Debrecen, Hungary

<sup>c</sup> University of Debrecen, PhD school of Physics, H-4026, Debrecen, Hungary

<sup>d</sup> RIKEN Nishina Center, Wako, Saitama 351-0198, Japan

<sup>e</sup> Instituto de Estructura de la Materia, IEM-CSIC, E-28006 Madrid, Spain

<sup>f</sup> Grand Accélérateur National d'Ions Lourds, CEA/DRF-CNRS/IN2P3, Bd Henri Becquerel, F-14076 Caen, France

<sup>g</sup> Istituto Nazionale di Fisica Nucleare, Laboratori Nazionali di Legnaro, Legnaro I-35020, Italy

<sup>h</sup> Istituto Nazionale di Fisica Nucleare, Sezione di Padova, Padova I-35131, Italy

<sup>i</sup> Dipartimento di Fisica dell'Università degli Studi di Padova, Padova I-35131, Italy

<sup>j</sup> Eötvös Loránd University, Institute of Physics, H-1053 Budapest, Hungary

<sup>k</sup> Faculty of Physics, VNU Hanoi University of Science, 334 Nguyen Trai, Thanh Xuan, Hanoi, Viet Nam

<sup>l</sup> Extreme Light Infrastructure-Nuclear Physics (ELI-NP) & Horia Hulubei National Institute for Physics and Nuclear Engineering (IFIN-HH), Str. Reactorului 30, Bucharest-Măgurele 077125, Romania

<sup>m</sup> Centre d'Etudes Nucléaires de Bordeaux-Gradignan, UMR 5797 Université de Bordeaux CNRS/IN2P3, 19 Chemin du Solarium, CS10120, 33175 Gradignan Cedex, France

<sup>n</sup> Department of Physics, University of Surrey, Guildford GU2 7XH, United Kingdom

<sup>o</sup> Research Center for Nuclear Physics, Osaka University, Ibaraki, Osaka 567-0047, Japan

<sup>p</sup> Department of Physics, Osaka University, Toyonaka, Osaka 560-0043, Japan

<sup>q</sup> Centro de Investigación en Física Nuclear y Espectroscopia de Neutrones CEFNEN, Comisión Chilena de Energía Nuclear, Nueva Bilbao 12501, Las Condes, Santiago, Chile

<sup>r</sup> Institute of Nuclear Physics, University of Cologne, D-50937 Cologne, Germany

<sup>s</sup> Physik Department E12, Technische Universität München, D-85748 Garching, Germany

<sup>t</sup> National Institute for Physics and Nuclear Engineering IFIN-HH, P.O. Box MG-6, Bucharest-Măgurele, Romania

<sup>u</sup> Department of Physics, Istanbul University, Istanbul 34134, Turkey

<sup>v</sup> Department of Natural Sciences, Tokyo City University, Setagaya-ku, Tokyo 158-8557, Japan

<sup>w</sup> Department of Physics, Tokyo University of Science, Noda, Chiba 278-8510, Japan

<sup>x</sup> CEA Saclay, IRFU, SPhN, 91191 Gif-sur-Yvette, France

<sup>y</sup> Grand Accélérateur National d'Ions Lourds, B.P. 55027, F-14076 Caen Cedex 05, France

<sup>z</sup> Department of Physics, University of York, Heslington, York YO10 5DD, United Kingdom

<sup>aa</sup> Department of Physics, University of Hong Kong, Pokfulam, Hong Kong

<sup>ab</sup> GSI, Planckstrasse 1, D-64291 Darmstadt, Germany

\* Corresponding author.

E-mail addresses: [algora@ific.uv.es](mailto:algora@ific.uv.es) (A. Algóra), [gabor.kiss@atomki.mta.hu](mailto:gabor.kiss@atomki.mta.hu) (G.G. Kiss).

## ARTICLE INFO

## Article history:

Received 21 October 2021

Received in revised form 12 March 2022

Accepted 19 April 2022

Available online 27 April 2022

Editor: D.F. Geesaman

## Keywords:

Beta decay of  $^{70}\text{Kr}$ 

pn pairing

GT strength distribution

Pseudo-SU(4) symmetry

QRPA calculations

## ABSTRACT

The  $\beta$ -decay of the even-even nucleus  $^{70}\text{Kr}$  with  $Z = N + 2$ , has been investigated at the Radioactive Ion Beam Factory (RIBF) of the RIKEN Nishina Center using the BigRIPS fragment separator, the ZeroDegree Spectrometer, the WAS3ABI implantation station and the EURICA HPGe cluster array. Fifteen  $\gamma$ -rays associated with the  $\beta$ -decay of  $^{70}\text{Kr}$  into  $^{70}\text{Br}$  have been identified for the first time, defining ten populated states below  $E_{\text{exc}} = 3300$  keV. The half-life of  $^{70}\text{Kr}$  was derived with increased precision and found to be  $t_{1/2} = 45.19 \pm 0.14$  ms. The  $\beta$ -delayed proton emission probability has also been determined as  $\varepsilon_p = 0.545(23)\%$ . An increase in the  $\beta$ -strength to the yrast  $1^+$  state in comparison with the heaviest  $Z = N + 2$  system studied so far ( $^{62}\text{Ge}$  decay) is observed that may indicate increased np correlations in the  $T = 0$  channel. The  $\beta$ -decay strength deduced from the results is interpreted in terms of the proton-neutron quasiparticle random-phase approximation (pnQRPA) and also with a schematic model that includes isoscalar and isovector pairing in addition to quadrupole deformation. The application of this last model indicates an approximate realization of pseudo-SU(4) symmetry in this system.

© 2022 The Author(s). Published by Elsevier B.V. This is an open access article under the CC BY license (<http://creativecommons.org/licenses/by/4.0/>). Funded by SCOAP<sup>3</sup>.

## 1. Introduction

The basic ingredients of nuclei, protons and neutrons, can be considered as two states of the same particle, the nucleon. This assumption, introduced by Heisenberg [1], later gained great relevance in nuclear physics, since it led to the concept of isospin symmetry by assigning an isospin  $T = 1/2$  to a nucleon with projection  $T_z = -1/2$  for a proton and  $T_z = +1/2$  for a neutron.

Isospin symmetry is assumed to be only slightly broken. Departure from it, due to electromagnetic effects and possible isospin violating components of the strong interaction, can provide information about isospin mixing, isospin-symmetry breaking and the presence of three-body nuclear forces.

This paper presents the first  $\beta$ -decay study of the  $T_z = -1$   $^{70}\text{Kr}$  nucleus into the  $N = Z$  daughter  $^{70}\text{Br}$  using state-of-the-art instrumentation. This decay represents the heaviest and most exotic case of this kind studied so far and provides information to help clarify long-standing as well as very recent questions related to isospin symmetry, nuclear deformation and proton-neutron (pn) pairing.

One timely question that can be directly related to our  $\beta$ -decay study was raised very recently by the work of Lenzi et al. [2] in relation to the work of Wimmer et al. [3]. In Wimmer et al. the  $B(E2; 0_{gs}^+ \rightarrow 2_1^+)$  reduced transition probability in  $^{70}\text{Kr}$  is extracted from an inelastic scattering study. Comparison of the deduced transition matrix element ( $M_p(E2)$ ) with those of  $^{70}\text{Br}$  and  $^{70}\text{Se}$ , the other members of the  $A = 70$  isospin triplet, reveals a  $3\sigma$  deviation from the expected linear trend of  $M_p(E2)$  as a function of  $T_z$ . This result is interpreted as the first violation of isospin symmetry at the  $3\sigma$  level in  $E2$  transition matrix elements. As a possible explanation of the  $M_p$  anomaly a shape change between the  $^{70}\text{Kr}$  and  $^{70}\text{Se}$  mirror nuclei is proposed, in contradiction to what nuclear models predict [3].

Lenzi et al. [2] provide an alternative explanation for the anomaly. They perform state-of-the-art shell-model calculations for the members of the  $A = 70$  triplet, and find only a small departure from the expected linear trend for  $M_p$ . They identify the  $^{70}\text{Br}$  matrix element as the source of the possible discrepancy, not the value for  $^{70}\text{Kr}$  as suggested by Wimmer et al. They also argue that a possible explanation for the anomalous value of  $M_p$  in  $^{70}\text{Br}$  could be the existence of a hitherto undetected  $1^+$  state lying below the yrast  $2^+$  state. A  $\beta$ -decay study like the one presented here can be instrumental in providing an answer to this possible explanation of the  $M_p$  anomaly due to its high sensitivity to identify  $1^+$  states in  $^{70}\text{Br}$ .

The  $^{70}\text{Kr}$  decay is also of interest from the perspective of nuclear shapes and shape coexistence. Nuclei around  $A = 80$  are

characterized by drastic shape changes, which depend on the occupancy of the proton and neutron orbitals in a region dominated by prolate and oblate shell gaps and low level density. Wimmer et al. [3] interpret the dramatic change found in the  $B(E2; 0_{gs}^+ \rightarrow 2_1^+)$  value between  $^{70}\text{Se}$  and  $^{70}\text{Kr}$  as the result of a possible change of shape between the mirror partners, indicating a larger deformation in  $^{70}\text{Kr}$  than in  $^{70}\text{Se}$ .

It is therefore of interest to obtain additional information on the deformation of the ground state of  $^{70}\text{Kr}$ . The determination of the shape of the ground state of a nucleus is not an easy task, especially for exotic nuclei. But, in particular cases, the ground-state shape of the parent nucleus can be inferred from a comparison of the experimental  $\beta$ -strength with theory. This is possible if the theoretical calculations show different patterns depending on the assumed shape of the parent state. The idea, originally proposed in [4] and further studied in [5–7], has been applied successfully in the  $A \approx 70$  and  $A \approx 190$  regions [8–12]. The theoretical strength distributions of the  $\beta$ -decay of  $^{70}\text{Kr}$  show slight differences depending on the shape of the ground state [13]. Therefore, under the assumption that most of the  $\beta$ -strength is seen experimentally, it will provide us with additional information on the nuclear shape. It should be noted that shape studies in this region are challenging theoretically as already discussed in [2,11] and do not always provide a definite conclusion.

Another motivation of the present work is the search for possible signatures of proton-neutron (pn) pairing. The ground states of many nuclei are very well described in terms of superfluid condensates, in which pairs of nucleons are formed like Cooper pairs of electrons in superconductors [14]. The original theory of nucleon-pair correlations only included Cooper pairs of identical nucleons and no pn pairs. Already in the 1960s, however, it was recognized that this pairing theory is incomplete and that pn pairs should be included. This generalization was performed in stages, first by including pp, nn and pn pairs coupled to isospin  $T = 1$  and later by adding pn pairs coupled to isospin  $T = 0$ . To date, only a nuclear superconducting phase associated with Cooper pairs of identical nucleons has been unambiguously observed. Whether there also exists a deuteron-like condensate based on strongly correlated isoscalar ( $T = 0$ ) pn pairs remains an open question that still attracts great interest (see [15] and references therein). One inherent difficulty in these studies is that, to exploit the short-range character of the nuclear force and to form  $T = 0$  correlated Cooper pairs, nucleons must occupy orbits within the same valence shell, so studies must be performed along the  $N = Z$  line.

Experimentally there are several possibilities to explore the effects of  $T = 0$  pn pairing [16], which range from rotational alignment [17] and changes in level densities in  $N = Z$  nuclei [18]

to effects on binding energies, pairing vibrations and two-particle transfers (for a recent review, see [19]). One further possibility, discussed in [16,19], is related to the effect of pn pairing on  $\beta$ -decay rates [20–23], which is addressed here through the study of the  $\beta$ -decay of  $^{70}\text{Kr}$ . The  $^{62}\text{Ge}$  decay [24] is the heaviest similar system studied up to now and provides no evidence of enhanced Gamow-Teller transitions. However, an enhancement of  $T = 0$  pn correlations with increasing mass number  $A$  is still possible, as argued in [16,25], which justifies the study of heavier beta-decaying systems near the  $N = Z$  line.

A good starting point for a discussion of  $T = 0$  and  $T = 1$  pairing modes and their effect on  $\beta$ -decay is Wigner's supermultiplet scheme [26] since isoscalar and isovector pairing enter on an equal footing in this model and its underlying SU(4) symmetry leads to selection rules in Gamow-Teller (GT)  $\beta$ -decay. Along the  $N = Z$  line, for the  $\beta$ -decay from an  $Z = N + 2$  parent into an  $N = Z$  daughter, SU(4) symmetry predicts superallowed transitions to the yrast  $1^+$  state of an odd-odd nucleus and forbidden ones into an even-even nucleus [23]. While, except in the lightest nuclei, SU(4) symmetry is strongly broken mainly as a consequence of the spin-orbit interaction, in certain mass regions a *pseudo*-SU(4) symmetry might be appropriate because of a small *pseudo* spin-orbit splitting [27,28]. Specifically, in nuclei above  $^{56}\text{Ni}$  it may arise by treating the dominant  $2p_{1/2}$ ,  $2p_{3/2}$  and  $1f_{5/2}$  orbitals as a *pseudo*- $sd$  shell. It should be stressed that the GT operator is *not* a generator of the *pseudo*-SU(4) algebra and therefore the usual SU(4) selection rules do not apply in a *pseudo* shell. As shown in Ref. [29], the  $^{58}\text{Zn} \rightarrow ^{58}\text{Cu}$   $\beta$ -decay agrees qualitatively with the *pseudo*-SU(4) predictions but a similar analysis for higher mass numbers has not been carried out so far.

The  $\beta$ -decay of  $^{70}\text{Kr}$  is also of relevance for the astrophysical rp-process [30]. This work contributes to the experimental determination of the decay properties of  $^{70}\text{Kr}$  as part of a programme aimed at providing reliable data on the  $\beta$ -decay of waiting points and neighbouring nuclei involved in the rp-process [31–33]. The main goal is to improve the quality of the nuclear physics input in astrophysical network calculations and to validate theoretical calculations applicable to the prediction of unknown nuclear properties. Up to now, very little was known about the  $\beta$ -decay of  $^{70}\text{Kr}$ : the half-life of the decay has been determined at CERN ISOLDE from the time distribution of the emitted  $\beta$ -particles [34], and no states populated in the  $\beta$ -decay were known prior to this work.

## 2. Experimental approach

The experiment was performed at the RIKEN Nishina Center (Wako-shi, Saitama, Japan). The  $^{70}\text{Kr}$  ions were produced by fragmentation of a  $^{78}\text{Kr}$  primary beam with  $I_{\text{beam}} \sim 40$  pA average intensity and  $E_{\text{beam}} = 345$  MeV/nucleon energy impinging on a 5 mm thick  $^9\text{Be}$  target. Identification of particles with the atomic number ( $Z$ ) and the mass-to-charge ratio ( $A/q$ ) was achieved on the basis of the  $\Delta E$ -TOF- $B\rho$  method, in which the energy loss ( $\Delta E$ ), time of flight (TOF), and magnetic rigidity ( $B\rho$ ) were measured using detectors along the path of the ions in the BigRips fragment separator [35].

About  $1.6 \times 10^6$   $^{70}\text{Kr}$  isotopes were produced, then implanted into WAS3ABI [36], which consisted of a compact stack of three double-sided silicon strip detectors (DSSSD). Each DSSSD had a thickness of 1 mm with an active area segmented into 60 and 40 strips (corresponding to 2400 pixels with an active area of  $1 \times 1$  mm<sup>2</sup> each) on each side in the horizontal and vertical directions, respectively. The DSSSDs were also used to detect the  $\beta$ -particles and the  $\beta$ -delayed protons. The full energy ranges for the light particles in the X and Y strips were 4 MeV and 10 MeV. The  $\gamma$ -rays emitted following the  $\beta$ -decay of the implanted nu-

clei were detected using the EURICA (Euroball-RIKEN Cluster Array) spectrometer [37] which consisted of 84 HPGe crystals arranged in twelve clusters at a nominal distance of 22 cm from the centre of WAS3ABI. The efficiency of the  $\gamma$ -ray array was determined using calibrated  $^{60}\text{Co}$ ,  $^{133}\text{Ba}$  and  $^{152}\text{Eu}$  sources [37]. The absolute  $\gamma$ -peak detection efficiency was about 8% at 1332 keV, the energy of the  $\gamma$ -ray from the  $^{60}\text{Co}$  calibration source.

The event selection criteria employed in the analysis are discussed in detail in [38,39]. Implantation events in WAS3ABI were correlated in time with decay events taking place in the same pixel where the implantation event was observed. In the analysis of the experimental data the maximum time difference between an implantation and the corresponding detection of a  $\beta$ -particle was fixed at 20 s and the  $\beta$ -delayed  $\gamma$ -events were recorded up to 800 ns after the identified  $\beta$ -events.

The half-life of  $^{70}\text{Kr}$  was determined in a previous experiment with large uncertainty ( $\pm 15\%$ ) [34]. In the present work it was derived using two methods. The half-life of  $^{70}\text{Kr}$  was first determined from the time distribution of implantation- $\beta$  ( $i$ - $\beta$ ) correlations fitted with the Bateman-formula and a background term, extracted from a linear fit to the backward-time distribution of  $i$ - $\beta$  correlations. The Bateman-formula included the decays of  $^{70}\text{Kr}$  and  $^{70}\text{Br}$  assuming a value of  $78.42 \pm 0.51$  ms [38] for the half-life of  $^{70}\text{Br}$ . The  $\beta$ - and the  $\beta$ -delayed proton- events were distinguished by applying an energy cut at  $E_{\text{cut}} = 1400$  keV on the high gain WAS3ABI events; so particles with energies lower than  $E_{\text{cut}}$  were identified as  $\beta$ -particles and the rest as involving protons. A publication with more details on the data analysis of the proton branch is in preparation [40]. A value for the half-life of  $^{70}\text{Kr}$  was also extracted from the decay curves of the strong  $\beta$ -delayed  $\gamma$ -transitions listed in Table 1 (observed at  $E_{\gamma} = 933, 1120, 1493, 1574, 1630, 2230, 2306, 2508$  and  $2563$  keV). The time distributions of the implantation- $\beta$ - $\gamma$  ( $i$ - $\beta$ - $\gamma$ ) coincidence events for these transitions were summed and fitted with the sum of an exponential function and a constant background. In both approaches, the systematic uncertainties were investigated by varying the fit parameters. Fig. 1 shows the time distribution of  $i$ - $\beta$  (left) and  $i$ - $\beta$ - $\gamma$  (right) correlations, the green and blue lines correspond to individual activities and the red ones to the background, respectively. The resulting values for the half-life were found to be  $t_{1/2} = 45.19 \pm 0.14$  ms ( $i$ - $\beta$ ) and  $t_{1/2} = 44.9 \pm 1.1$  ms ( $i$ - $\beta$ - $\gamma$ ), respectively. The half-life value obtained from  $i$ - $\beta$  correlations shows about 50-fold improvement in precision, compared to the earlier result,  $40 \pm 6$  ms [34].

The  $\beta$ -decay of  $^{70}\text{Kr}$  proceeds to states in  $^{70}\text{Br}$ . As  $Q_{\varepsilon p} > 0$ , beta-delayed proton emission is also allowed leading to  $^{69}\text{Se}$ . The proton-emission probability was found to be  $\varepsilon_p = 0.545(23)\%$ , determined from an exponential plus linear background fit to the  $i$ -proton time distributions. Gamma-rays emitted in the de-excitation of states populated in the  $\beta$ -decay were first identified by comparing the half-life obtained from  $i$ - $\beta$ - $\gamma$  correlations with the value previously obtained from the  $i$ - $\beta$  correlations. From the identified  $\gamma$ -rays only one  $\gamma$ -ray ( $E_{\gamma} \approx 933$  keV) was known previously and assigned to the de-excitation of the 1<sup>st</sup> excited state of  $^{70}\text{Br}$  [41]. Fig. 2 shows the measured  $\gamma$ -spectrum in coincidence with  $^{70}\text{Kr}$  implants. Altogether 15  $\gamma$ -transitions, listed in Table 1 were identified for the first time. The level-scheme, shown in Fig. 3, was deduced from  $\gamma$  -  $\gamma$  coincidence events. This was done by first identifying gamma rays populating the first excited state in  $^{70}\text{Br}$  by gating on the  $E_{\gamma} = 933.4(2)$  keV  $\gamma$ -line. Then, direct transitions connecting the newly found excited states with the ground state were sought. In the next step, a gate was set on each of the newly found transitions to look for additional cascades. Finally, intense  $\gamma$ -rays in coincidence with the 511 keV annihilation  $\gamma$ -line and with half-lives in agreement with the  $t_{1/2}$  value derived from the  $i$ - $\beta$  correlations were placed in the level

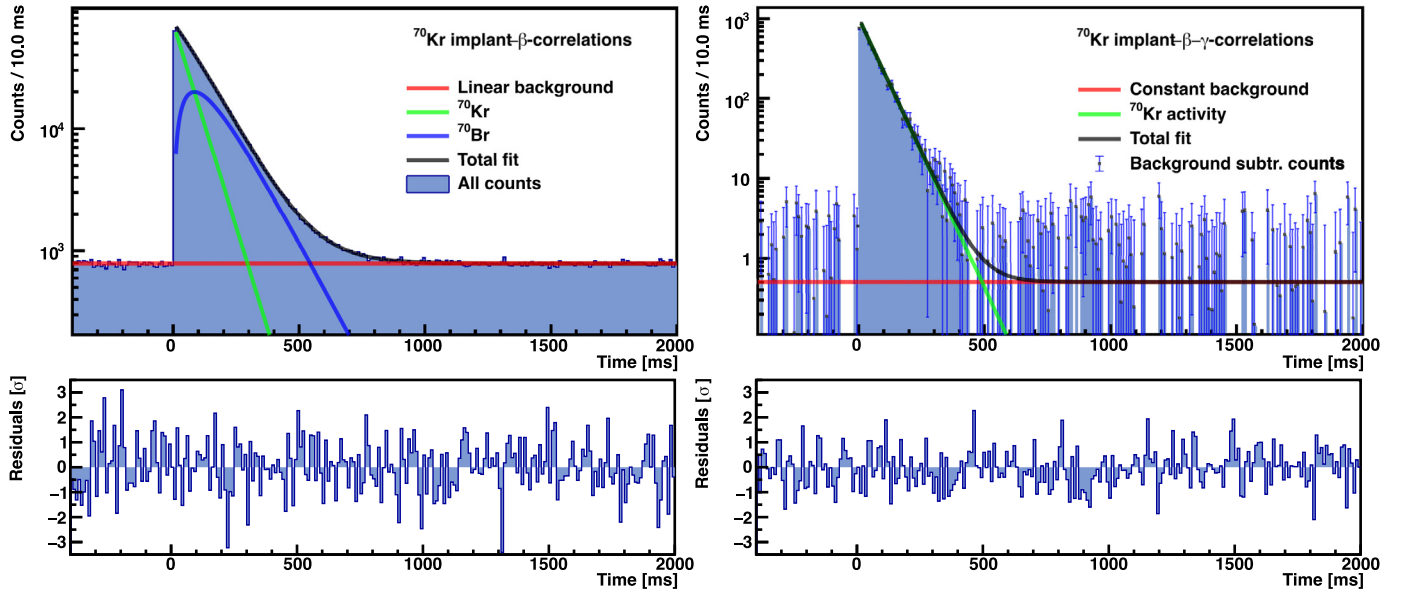


**Fig. 1.** The time distribution of  $i$ - $\beta$  (left) and  $i$ - $\beta$ - $\gamma$  (right) correlations. The fitting function for the  $i$ - $\beta$  time distribution includes the Bateman formula for the  $^{70}\text{Kr}$  and  $^{70}\text{Br}$  decays, assuming a value of  $78.42 \pm 0.51$  ms [38] for the half-life of  $^{70}\text{Br}$  and a background term extracted from a linear fit to the backward-time distribution of  $i$ - $\beta$  correlations. The black, green, blue and red curves correspond to the total fit, the resulting partial activities and to the background, respectively. In the case of the  $i$ - $\beta$ - $\gamma$  correlations the total fit is the sum of the identified, high-intensity  $\gamma$ -peaks' activities which is calculated from the subtraction of the time distribution of the total area of the peaks, the Compton-background activity, and a constant background. The black, green and red curves correspond to the total fit, the sum of the  $\gamma$ -peak activities and the background, respectively.

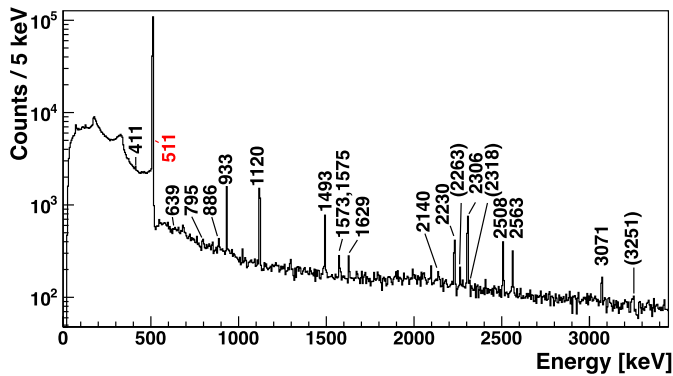


**Fig. 2.** Energy spectrum of the  $\beta$ -delayed  $\gamma$ -rays from  $^{70}\text{Kr}$ . The peaks, definitely assigned to the  $\beta$ -decay of  $^{70}\text{Kr}$  are marked with black, bold labels and placed in the level scheme. The energies of the three  $\gamma$ -rays assigned to the decay of levels in  $^{70}\text{Br}$  with lower confidence are labeled between brackets.

scheme. The  $\gamma$ -ray intensities were derived by taking into account the known detection efficiencies and background subtracted peak areas. During the analysis we also found indications of the existence of two more states, and three more transitions. They are shown in Fig. 3 with their energies in parentheses and the levels represented by dashed lines and the transitions by grey arrows, respectively.

In order to assign spin and parities to the states identified, we take into account that the  $\beta$ -decay of the  $J^+ = 0^+$ ,  $T = 1$  ground state of  $^{70}\text{Kr}$  populates the  $0^+$  isobaric analog state in  $^{70}\text{Br}$  through a super-allowed Fermi transition and  $1^+$  states through allowed Gamow-Teller transitions. We have also assumed that the state previously identified in  $^{70}\text{Br}$  in in-beam studies at 933 keV is a  $2^+$  state. This assumption is based on the DCO measurements of [41,42] and the similar excitation energy of the  $2^+$  isobaric analogue state at 944 keV in  $^{70}\text{Se}$  [41]. Then, spins and parities have been assigned to the newly identified levels based on the intensity of the apparent  $\beta$ -feeding and their gamma de-excitation pattern to the levels with previously assigned spins and parities (the  $0^+$

ground state and the  $2^+$  state at 933 keV). It was not possible to study the angular correlations of the gamma rays because of the limited statistics.

Based on these criteria we have identified the 1120 and 2306 keV levels as firm  $1^+$  states, which show the largest apparent  $\beta$ -feeding (among the excited states), the smallest logft values and strong  $\gamma$ -transitions to the  $0^+$  ground state. States at 1493, 2230 keV which show smaller beta feeding and similar decay patterns are conservatively assigned ( $1^+$ ). Similarly, ( $1^+$ ) is assigned to the level at 3071 keV, which has a similar decay pattern to the 1120, 1493 and 2306 keV levels (only one  $\gamma$ -transition to the ground state) but a weaker apparent feeding. The state at 1344 keV is identified as a possible  $0^+$ , since it does not show a strong apparent  $\beta$ -feeding and it is only connected to the  $2^+$  state at 933 keV. This state (at 1344 keV) also receives  $\gamma$ -feeding from the 2230 keV state previously identified tentatively as  $1^+$ . The state at 1573 keV is tentatively assigned as  $1^+$ , since it receives weak apparent  $\beta$ -feeding, and decays to the 933 keV  $2^+$  state and the  $0^+$  ground state. Similarly ( $1^+$ ) is assigned to the state at 2140 keV based on the  $\gamma$ -transition decay pattern, which connects it to the ground state and to the state previously assigned tentatively as  $0^+$  at 1344 keV. This state also has a weak apparent  $\beta$ -feeding. And finally ( $1^+$ ) is also assigned to levels at 2508 and 2563 keV, which present relatively strong direct  $\beta$ -feeding and are connected to the 933 keV  $2^+$  state and the  $0^+$  ground state. It is worth noting that we do not see gamma transitions between the assigned  $1^+$  and ( $1^+$ ) states, which is an indication of the correctness of the assignment based on the quasi-rule that states that  $\Delta T = 0$  M1 transitions in self-conjugate nuclei are expected to be weaker by a factor of 100 than the average M1 transition strength [43].

To derive the  $B(\text{GT})$  values the absolute number of the  $\beta$ - $\gamma$  coincidence events, corresponding to the decay of  $^{70}\text{Kr}$ , has to be known. The total number of  $\beta$ -particles emitted in the  $\beta$ -decay of  $^{70}\text{Kr}$  was determined by integrating the appropriate component of the  $i$ - $\beta$  correlations in the fit to the Bateman equation. The resulting  $B(\text{GT})$  strengths are listed in Table 1. It should be noted, however, that these experimental  $B(\text{GT})$  values represent an



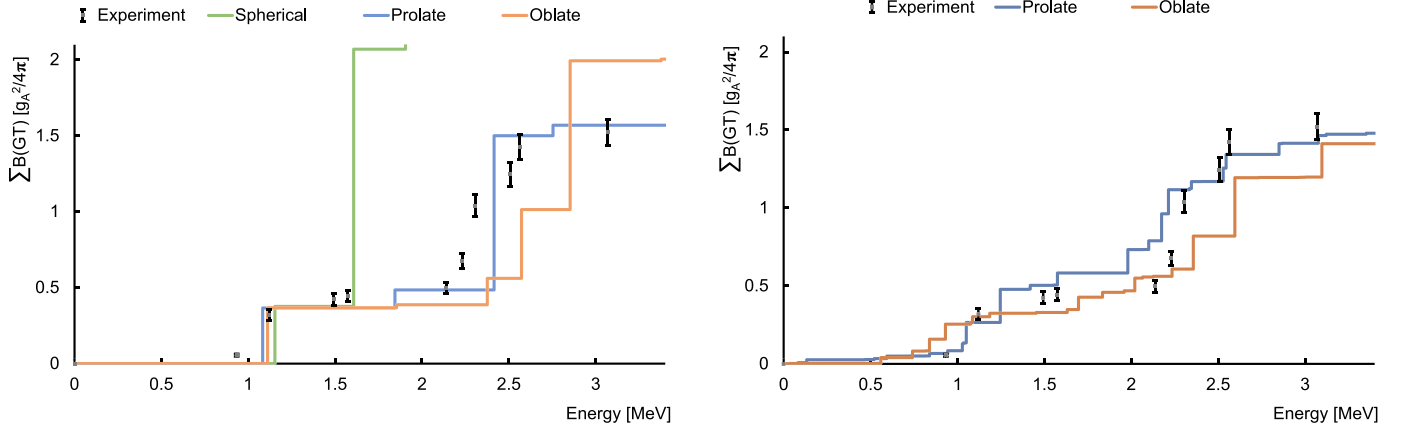


**Fig. 4.** Distribution of GT strength in the  $^{70}\text{Kr} \rightarrow ^{70}\text{Br}$  decay. The experimental  $B(\text{GT})$  distribution and its uncertainty are indicated in grey symbols. Please note that the experimental accumulated strength includes the contribution of all excited levels placed in the level scheme. The theoretical  $B(\text{GT})$  distribution in the left-hand panel is calculated with the Hamiltonian (1) with  $\epsilon_s = 0.500$  MeV for zero (green line,  $\kappa = 0$ ,  $g_0 = 10$ ,  $g_1 = 21$ ), prolate (blue line,  $\kappa = 0.015$ ,  $g_0 = 23$ ,  $g_1 = 34$ ) or oblate (orange line,  $\kappa = 0.030$ ,  $g_0 = 16$ ,  $g_1 = 26$ ) quadrupole deformation, with  $\kappa$  in MeV and  $g_i$  in  $\text{MeV fm}^2$ . The calculated GT strengths are quenched by  $q^2 = (0.74)^2$ , a typical value in the  $pf$  shell [50]. The right-hand panel shows the results from prolate and oblate QRPA calculations (see text).

the strengths of the delta interaction in the isoscalar and isovector channels, respectively, and  $\kappa$  is the strength of the quadrupole interaction in terms of an operator  $\sum_i Q_{\pm}(i)$  with a plus or minus sign, corresponding to prolate or oblate deformation. The Hamiltonian (1) assumes degenerate  $2p_{3/2}$  and  $1f_{5/2}$  orbitals and as a result the pseudo-orbital angular momentum  $\tilde{L}$  and the pseudo-spin  $\tilde{S}$  are conserved quantum numbers for all parameter values. If  $g_0 = g_1$ , it additionally has a pseudo-SU(4) symmetry.

The pseudo- $LS$  Hamiltonian (1), although schematic, helps to provide an intuitive understanding of how the  $B(\text{GT})$  distribution depends on the single-particle structure, the isoscalar and isovector strengths and the deformation [49]. This is illustrated in Fig. 4 (left), which shows the  $B(\text{GT})$  distributions obtained assuming no, prolate or oblate quadrupole deformation. There is only a weak dependence of the GT strength on  $\epsilon_s$ , which is kept fixed. The strengths  $g_i$  are chosen as to reproduce the energy differences  $E_x(2_1^+) - E_x(0_1^+)$  and  $E_x(1_1^+) - E_x(0_1^+)$  in  $^{70}\text{Br}$ . In the case of no deformation too much strength is calculated at low excitation energy. The quadrupole interaction pushes this strength to higher energies but it is difficult to distinguish between the effects of prolate and oblate deformation. It is seen in Fig. 4 that in all cases some GT strength is concentrated in the  $1_1^+$  level. This finding can be understood as follows. As shown in [29] and references therein, matrix elements between eigenstates of a pseudo- $LS$  Hamiltonian calculated with the (quenched) GT operator  $\frac{q}{\sqrt{2}} \sum_k \sigma_{\mu}(k) \tau_{\pm 1}(k)$  are identical to those between eigenstates of an  $LS$  Hamiltonian calculated with a transformed operator of the form

$$-\frac{q}{\sqrt{2}} \sum_{k=1}^A \left\{ \frac{1}{3} \sigma_{\mu}(k) \tau_{\pm 1}(k) + \frac{4\sqrt{2\pi}}{3} [Y_2(k) \times \sigma(k)]_{\mu}^{(1)} \tau_{\pm 1}(k) \right\}. \quad (2)$$

The first piece of the transformed operator,  $\frac{1}{3} \bar{\sigma} \bar{\tau}$ , induces the GT strength to the  $1_1^+$  level. Although SU(4) symmetry is broken because  $g_0 \neq g_1$ , almost all  $\Delta L = 0$  GT strength is concentrated in the transition to  $1_1^+$ , as is the case in SU(4). Because of the factor  $\frac{1}{3}$  in the transformed operator, the strength is close to one-ninth of the SU(4) value, which in turn equals the Ikeda sum rule [51],  $B(\text{GT}; 0_1^+ \rightarrow 1_1^+) \approx \frac{2}{3} q^2$ . This is a robust prediction of pseudo-SU(4) symmetry, independent of the details of the calculation. This predicted feature agrees with the GT strength observed in  $A = 58$  and  $A = 70$ , but not in the intermediate systems, and one may there-

fore conjecture a return or a restoration of the pseudo-SU(4) symmetry as  $A$  increases. In contrast, the distribution of the  $\Delta L = 2$  strength generated by the second piece of the transformed operator,  $\frac{4\sqrt{2\pi}}{3} [Y_2 \times \bar{\sigma}]^{(1)} \bar{\tau}$ , is strongly influenced by the strengths of the delta interaction and by the deformation.

The experimental results can also be interpreted within a theoretical formalism based on the pn quasiparticle random-phase approximation (pnQRPA), previously used in the  $^{62}\text{Ge}$  case [24]. This is a beyond-mean-field calculation where the quasiparticle basis is obtained self-consistently from an axially deformed Hartree-Fock (HF) mean field, which is generated with density-dependent Skyrme interactions including pairing correlations between identical nucleons in the BCS approximation without explicit pn pairing.

The calculations reported in this work correspond to the force Sly4, which is a well tested and successful interaction throughout the whole nuclear chart. Constrained calculations are performed to investigate the energy of the nucleus as a function of the quadrupole deformation parameter  $\beta_2$ . We obtain for  $^{70}\text{Kr}$  two minima. The ground state appears for an oblate deformation  $\beta_2 = -0.22$ , whereas a second minimum is obtained with a prolate shape  $\beta_2 = 0.15$  at about 1 MeV above the ground state. The two minima are well separated by a spherical barrier of about 3 MeV [13].

Calculations of the energy distribution of the GT strength are performed for these two shapes in the HF + BCS + pnQRPA framework with residual spin-isospin interactions that include a proton-neutron pairing force in the  $J^{\pi} = 1^+$  coupling channel. Details of the formalism can be found in Refs. [5–7,52] and predictions for  $^{70}\text{Kr}$  have been published in Ref. [13]. The results shown in Fig. 4(right) are scaled with the same quenching factor ( $q^2 = (0.74)^2$ ) used in the calculations discussed previously. The figure compares the cumulative GT strength data with the results from the pnQRPA with the prolate and oblate shapes discussed above. In both cases one can see that the GT strength is concentrated around 1 MeV and between 2 and 2.5 MeV with magnitudes in fair agreement with experiment. The main spherical shells involved in the GT low-lying transitions are those in the vicinity of the Fermi surface, namely,  $2p_{3/2}$ ,  $1f_{5/2}$ , and  $2p_{1/2}$  in both protons and neutrons. Transitions between the proton and neutron deformed orbitals  $1/2^-$ ,  $3/2^-$ , and  $5/2^-$  are the building blocks of the GT strength. The only exceptions are the transitions between  $9/2^+$  orbitals from the  $1g_{9/2}$  spherical shell that contribute significantly around 1 MeV in the oblate case.

The differences observed between the results from oblate and prolate shapes are not large enough to favour one or the other and are comparable with the spread of the results obtained when other Skyrme forces different from SLy4 are used. On the one hand, at low excitation energies (below 2.3 MeV) a slightly better agreement can be noticed for an oblate shape in accordance with other model calculations [53,54] that predict an oblate ground state with  $\beta_2 = -0.33$  and  $\beta_2 = -0.28$  respectively for  $^{70}\text{Kr}$ . On the other hand, above 2.3 MeV the accumulated strength seems to be in slightly better agreement with the prolate deformation, but both calculations predict similar total beta strength values. The sharp increase in the accumulated strength at the lowest  $1^+$  state is also better reproduced by the prolate solution.

The interpretation of Wimmer et al. [3] of the  $M_p$  anomaly favours the larger deformation case (oblate in this framework) since larger collectivity in  $^{70}\text{Kr}$  is required to explain the change in the  $B(E2; 0_{gs}^+ \rightarrow 2_1^+)$  between  $^{70}\text{Se}$  and  $^{70}\text{Kr}$ . The difficulty of making a final statement about the shape from the present comparison with theory is not only a limitation of the pnQRPA calculations, it is also a limitation in state-of-the-art shell-model calculations as discussed in [2]. The calculations of Petrovici et al. [55] support the interpretation of Wimmer et al. because it is the only model that presently predicts a shape change between the isobars (the wave function of the ground state of  $^{70}\text{Kr}$  and  $^{70}\text{Br}$  is dominated by prolate components, while the oblate components are more important in  $^{70}\text{Se}$ ). This model also shows that shape mixing changes with spin and excitation energy being specific for each nucleus of the isovector triplet.

Even though the results from the pnQRPA model cannot decide the sign of the deformation, the results presented show that this formalism is able to describe the  $\beta$ -decay of  $^{70}\text{Kr}$  in terrestrial conditions, which is a necessary condition for the validation of the code for astrophysical applications.

We emphasize that the overall agreement of the experimental results with the calculated strength within pnQRPA framework that includes a residual pn pairing force but not at the mean-field level, does not allow us to draw a clear cut conclusion about the observed increase in the measured beta strength, when compared with the case of  $^{62}\text{Ge}$ , and to infer that it is induced by pn correlations in the  $T = 0$  channel. In the pnQRPA calculations the inclusion of the residual force in the particle-particle channel induces an enhancement of the strength and a shift to lower energies, but this effect is less important than that due to the force in the particle-hole channel. We would stress that the experimental result is clearly in line with what is expected in a heavier system approaching  $A \sim 80$  [16,25], where increased correlations in the  $T = 0$  pn channel are predicted.

Returning to the question raised Lenzi et al. [2], we do not see evidence of a  $1^+$  state below the  $2^+$  state at 934 keV in  $^{70}\text{Br}$  that could explain the anomalous behaviour of the  $M_p$  matrix elements. We have estimated the  $T(M1)/T(E2)$  branching ratio based on Ref. [2] and the  $1^+$  state should have been observed within the sensitivity limit of the present experiment. So, the reason for the anomaly observed in the  $M_p$  matrix elements [3] should be further explored.

In summary, we have presented the first detailed high-resolution study of the decay of the  $Z = N + 2$   $^{70}\text{Kr}$  nucleus. In this study, 10 states and 15  $\gamma$ -rays in  $^{70}\text{Br}$  have been identified clearly for the first time, thanks to the high beam intensities provided by the Radioactive Ion Beam Factory (RIBF) of the RIKEN Nishina Center and to the high sensitivity of the EURICA and WAS3ABi setups. No evidence for an yrast  $1^+$  state below the  $2_1^+$  state that could explain the  $M_p$  anomaly according to Ref. [2] was found. The decay of  $^{70}\text{Kr}$  has been interpreted in the framework of two models: a schematic pseudo- $LS$  model, which shows a restoration of pseudo-SU(4) symmetry based on the larger GT strength to the yrast  $1^+$  in  $^{70}\text{Br}$  in

this system compared to lighter ones, and a pnQRPA model that provides a good description of the accumulated GT strength. Relative to the observed  $\beta$ -decay of the lighter  $Z = N + 2$  nucleus,  $^{62}\text{Ge}$  [24,48], the GT strength to the  $1_1^+$  level in  $^{70}\text{Br}$  shows an approximate four-fold increase while the total GT strength increases by about a factor three. The results can also be of interest for astrophysical network calculations that simulate the rp-process.

## Declaration of competing interest

The authors declare that they have no known competing financial interests or personal relationships that could have appeared to influence the work reported in this paper.

## Acknowledgements

This work was supported by the National Research, Development and Innovation Fund of the Ministry for Innovation and Technology, Hungary with project no. TKP2021-NKTA-42 under the TKP2021 funding scheme. FM acknowledges the support of ANID/FONDECYT Regular 1171467 and ANID/FONDECYT Regular 1221364 national projects. This work was carried out at the RIBF operated by RIKEN Nishina Center and CNS, University of Tokyo. We acknowledge the EUROBALL Owners Committee for the loan of germanium detectors and the PreSpec Collaboration for the read-out electronics of the cluster detectors. This work was supported by the Spanish MICINN grants FPA2014-52823-C2-1-P, FPA2017-83946-C2-1-P (MCIU/AEI/FEDER); Ministerio de Ciencia e Innovación grant PID2019-104714GB-C21; Centro de Excelencia Severo Ochoa del IFIC SEV-2014-0398; *Junta para la Ampliación de Estudios* Programme (CSIC JAE-Doc contract) co-financed by FSE, by NKFIH (NN128072), the National Research, Development and Innovation Fund of Hungary Project No. K 128729 the STFC (UK) through Grant No. ST/P005314/, the PROMETEO/2019/007 project and by the ÚNKP-20-5-DE-02 New National Excellence Program of the Ministry of Human Capacities of Hungary and by the JSPS KAKENHI of Japan (Grant No. 25247045). G.G. Kiss acknowledges support from the János Bolyai research fellowship of the Hungarian Academy of Sciences. A. A. acknowledges partial support of the JSPS Invitational Fellowships for Research in Japan (ID: L1955) P. S. acknowledges support from MCI/AEI/FEDER,UE (Spain) under grant PGC2018-093636-B-I00.

## Appendix A. Supplementary material

Supplementary material related to this article can be found online at <https://doi.org/10.1016/j.physletb.2022.137123>.

## References

- [1] W. Heisenberg, *Z. Phys.* 77 (1932) 1.
- [2] S.M. Lenzi, A. Poves, A.O. Macchiavelli, *Phys. Rev. C* 104 (2021) L031306.
- [3] K. Wimmer, et al., *Phys. Rev. Lett.* 126 (2021) 072501.
- [4] I. Hamamoto, X.Z. Zhang, *Z. Phys. A* 353 (1995) 145.
- [5] P. Sarriguren, E. Moya de Guerra, A. Escuderos, A.C. Carrizo, *Nucl. Phys. A* 635 (1998) 55.
- [6] P. Sarriguren, E. Moya de Guerra, A. Escuderos, *Nucl. Phys. A* 658 (1999) 13.
- [7] P. Sarriguren, E. Moya de Guerra, A. Escuderos, *Nucl. Phys. A* 691 (2001) 631.
- [8] E. Nacher, et al., *Phys. Rev. Lett.* 92 (232501) (2004) 232501.
- [9] E. Poirier, et al., *Phys. Rev. C* 69 (2004) 034307.
- [10] A.B. Pérez-Cerdán, et al., *Phys. Rev. C* 88 (2013) 014324.
- [11] J.A. Briz, et al., *Phys. Rev. C* 92 (2015) 054326.
- [12] E. Estevez, et al., *Phys. Rev. C* 92 (2015) 044321.
- [13] P. Sarriguren, *Phys. Rev. C* 83 (2011) 025801.
- [14] A. Bohr, B.R. Mottelson, D. Pines, *Phys. Rev.* 110 (1958) 936.
- [15] A.L. Goodman, *Adv. Nucl. Phys.* 11 (1979) 263.
- [16] A.L. Goodman, *Phys. Rev. C* 60 (1999) 014311.
- [17] G. de Angelis, et al., *Phys. Lett. B* 415 (1997) 217.
- [18] K. Muhlhans, et al., *Z. Phys. A* 313 (1983) 133.

- [19] S. Frauendorf, A.O. Macchiavelli, *Prog. Part. Nucl. Phys.* 78 (2014) 24.
- [20] M. Cheoun, et al., *Nucl. Phys. A* 587 (1995) 301;  
G. Pantis, et al., *Phys. Rev. C* 53 (1996) 695.
- [21] F. Iachello, in: *Proc. Int. Conf. on Perspectives for the IBM, Padova, Italy, 1994*, p. 1.
- [22] F. Iachello, Yale University, preprint YCTP-N13-88.
- [23] P. Halse, B.R. Barrett, *Ann. Phys. (N. Y.)* 192 (1989) 204.
- [24] E. Grodner, et al., *Phys. Rev. Lett.* 113 (2014) 092501.
- [25] J. Jänecke, T.W. O'Donnell, *Phys. Lett. B* 605 (2005) 87.
- [26] E. Wigner, *Phys. Rev.* 51 (1937) 106.
- [27] A. Arima, M. Harvey, K. Shimizu, *Phys. Lett. B* 30 (1969) 517.
- [28] K.T. Hecht, A. Adler, *Nucl. Phys. A* 137 (1969) 129.
- [29] P. Van Isacker, O. Juillet, F. Nowacki, *Phys. Rev. Lett.* 82 (1999) 2060.
- [30] H. Schatz, et al., *Phys. Rev. Lett.* 86 (2001) 3471.
- [31] R.K. Wallace, S.E. Woosley, *Astrophys. J. Suppl. Ser.* 45 (1981) 389.
- [32] H. Schatz, et al., *Phys. Rep.* 294 (1998) 167.
- [33] A. Parikh, et al., *Prog. Part. Nucl. Phys.* 69 (2013) 225.
- [34] M. Oinonen, et al., *Phys. Rev. C* 61 (2000) 035801;  
G. Guerdal, E.A. McCutchan, *Nucl. Data Sheets* 136 (2016) 1.
- [35] N. Fukuda, et al., *Nucl. Instrum. Methods B* 317 (2013) 323.
- [36] S. Nishimura, *Prog. Theor. Exp. Phys.* (2012) 03C006.
- [37] P.-A. Söderström, et al., *Nucl. Instrum. Methods B* 317 (2013) 649.
- [38] A. Morales, et al., *Phys. Rev. C* 95 (2017) 064327.
- [39] A. Vitéz-Sveicz, et al., *Acta Phys. Pol.* 51 (3) (2020) 587–594.
- [40] A. Vitéz-Sveicz, et al., in preparation.
- [41] G. de Angelis, et al., *Eur. Phys. J. A* 12 (2001) 51.
- [42] D.G. Jenkins, et al., *Phys. Rev. C* 65 (2002) 064307.
- [43] *Isospin in Nuclear Physics*, chapter 5 by E.K. Warburton and J. Weneser, p. 185 D.H. Wilkinson (Ed.), North-Holland Publishing Company, Amsterdam, 1969, SBN7204 0155 0.
- [44] W.J. Huang, et al., *Chin. Phys. C* 45 (2021) 030002.
- [45] F. Osterfeld, *Rev. Mod. Phys.* 64 (1992) 491.
- [46] W.E. Ormand, B.A. Brown, *Phys. Rev. C* 52 (1995) 2455.
- [47] J.C. Hardy, et al., *Phys. Lett. B* 71 (1977) 307.
- [48] S.E.A. Orrigo, et al., *Phys. Rev. C* 103 (2021) 014324.
- [49] P. Van Isacker, in press.
- [50] Y. Fujita, et al., *Phys. Rev. Lett.* 112 (2014) 112502.
- [51] K. Ikeda, *Prog. Theor. Phys.* 31 (1964) 434.
- [52] P. Sarriguren, E. Moya de Guerra, A. Escuderos, *Phys. Rev. C* 64 (2001) 064306.
- [53] P. Möller, et al., *At. Data Nucl. Data Tables* 109–110 (2016) 1.
- [54] [http://www-phynu.cea.fr/science\\_en\\_ligne/carte\\_potentiels\\_microscopiques/carte\\_potentiel\\_nucleaire\\_eng.htm](http://www-phynu.cea.fr/science_en_ligne/carte_potentiels_microscopiques/carte_potentiel_nucleaire_eng.htm).
- [55] A. Petrovici, O. Andrei, A. Chilug, *Phys. Scr.* 93 (2018) 114001.